RESEARCH ARTICLE

Diffusion in a disk with inclusion: Evaluating Green's functions

Remus Stana, Grant Lythe[ID]*

Department of Applied Mathematics, University of Leeds, Leeds, United Kingdom

* grant@maths.leeds.ac.uk

Abstract

We give exact Green's functions in two space dimensions. We work in a scaled domain that is a circle of unit radius with a smaller circular "inclusion", of radius a, removed, without restriction on the size or position of the inclusion. We consider the two cases where one of the two boundaries is absorbing and the other is reflecting. Given a particle with diffusivity D, in a circle with radius R, the mean time to reach the absorbing boundary is a function of the initial condition, given by the integral of Green's function over the domain. We scale to a circle of unit radius, then transform to bipolar coordinates. We show the equivalence of two different series expansions, and obtain closed expressions that are not series expansions.

Introduction

Brownian motion is a common model of microscopic behaviour, such as that of intracellular molecules [1–4]. Depending on whether the mathematical interest is in statistics of many particles, or in single-particle properties such as mean hitting times, the diffusion, Laplace, or Poisson equation may need to be solved [5–8]. Absorption or reflection at surfaces is expressed in terms of boundary conditions. Green's function is the key to analytical solutions because it takes the shape of the domain and the boundary conditions into account. Quantities such as mean hitting times are obtained from it by standard integration, for any initial distribution [9–14]. It is also possible to model a surface with both absorbing and reflecting parts using Robin boundary conditions [15–17].

The domain we consider here is a circle of unit radius with a smaller circular "inclusion", of radius a, removed. The centre of the inclusion is displaced from the centre of the circle of unit radius by c, with $0 \leq c \leq 1 - a$. We consider the two cases where one circle is an absorbing boundary, the other is reflecting (reflecting inclusion inside a circular domain with absorbing boundary, and *vice versa*). In [14], the circle of unit radius was referred to as the cellular surface and the inclusion as the cell's nucleus. In two and three dimensions, Condamin *et al*. [18], constructed approximate Green's functions. Asymptotic and numerical methods can be used when there are multiple targets of different shapes in a two-dimensional region [19–22]. They are accurate when the targets are not too large, not too close to each other and not too close to the cellular surface. The functions given here are, however, exact without restriction on the size or position of the inclusion.
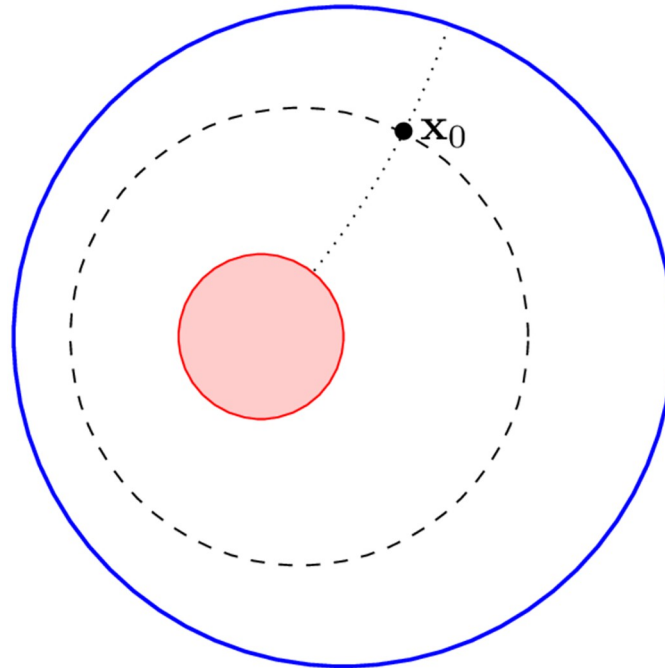
Fig 1. The domain is the interior of the unit circle (blue) with a circular inclusion (red). The initial position of a diffusing particle, $\mathbf{x}_0$, has bipolar coordinates τ_0, σ_0. The dashed circle is the set of points with $\tau = \tau_0$. The dotted arc is part of the set of points with $\sigma = \sigma_0$. $G_1(\mathbf{x}_0, \mathbf{x})$ is the solution of (4), constrained to be zero on the unit circle and to have normal derivative on the inclusion. $G_2(\mathbf{x}_0, \mathbf{x})$ is the solution of (4), constrained to be zero on the inclusion and to have normal derivative on the unit circle.

We use bipolar coordinates, τ and σ (Fig 1); the circle of unit radius has $\tau = \tau_2$ and the boundary of the inclusion has $\tau = \tau_1$, where

$$\tau_1 = \log\left(d/a + \sqrt{1 + (d/a)^2}\right), \qquad \tau_2 = \log\left(d + \sqrt{1 + d^2}\right) \tag{1}$$

and

$$d = \frac{1}{2c}\sqrt{\left(1 + a^2 - c^2\right)^2 - 4a^2}. \tag{2}$$

We calculate Green's functions on the rectangular domain in bipolar coordinates $\tau_2 \leq \tau \leq \tau_1$, $0 \leq \sigma \leq 2\pi$; mean exit times are calculated by integrating over the coordinates (τ, σ) [14].

The transformation from Cartesian to bipolar coordinates, (x, y) to (τ, σ), is a type of conformal transformation employed, for example, to express the electric potential between two parallel cylinders [5, 23]. Another example of a conformal transformation is the bilinear function

$$f(z) = \frac{z + \alpha}{z + \beta},$$

where $z = x + iy$. Circles are mapped to circles and, with suitable choices of α and β, two non-concentric circles can be mapped to two concentric ones. When one is the unit circle, $\alpha\beta = 1$ [24]. The bilinear transformation has been used to obtain solutions of Laplace's equation with absorbing boundaries on both circles [25, 26]. We may construct Green's functions in

nonconcentric domains from those in concentric domains, $\tilde{G}$, which are also series expansions [27], as $\tilde{G}(f^{-1}(z_0), f^{-1}(z))$. However, the integrals needed to calculate mean exit times have only been performed using bipolar coordinates [14].

Green's function $G(\mathbf{x}_0, \mathbf{x})$ is a symmetric function of two positions $\mathbf{x}_0$ and $\mathbf{x}$, where $\mathbf{x}_0$ is taken to be the position of a point charge or the initial condition of a diffusing particle. As a result, $G(\mathbf{x}_0, \mathbf{x})$ is proportional to $-\log|\mathbf{x} - \mathbf{x}_0|$ as $\mathbf{x} \to \mathbf{x}_0$. Writing it as a sum of singular and regular parts, and expressing both in bipolar coordinates [5, 28], Heyda was able to find a series expression for Green's function with absorbing boundaries. A different approach to the same problem [29], because the transformed domain is rectangular, is to expand Green's function in trigonometric eigenfunctions. The resulting series solution can be summed to yield an explicit expression involving Jacobi Theta functions [29]. Heyda's method has recently been applied to the problem where one circular boundary is absorbing and the other is reflecting [14]. Explicit exact solutions are useful, even when they are series, because they can be integrated to yield mean transport times, or expanded in small parameters to yield simple expressions, depending on the geometry and dynamics of the context of diffusion in confined geometries [8, 30–35].

Given a particle with diffusivity D, in a circle with radius R, the mean time to reach an absorbing boundary is a function of the initial condition, given by the integral of Green's function over the domain. Given R, we firstly scale to a circle of unit radius, then transform to bipolar coordinates. With the Jacobian factor of the transformation, $d^2/(\cosh \tau - \cos \sigma)^2$, the integral is written as

$$T(\mathbf{x}_0) = \frac{R^2}{D} \int_{\tau_2}^{\tau_1} \int_0^{2\pi} \frac{G(\mathbf{x}_0, \mathbf{x})d^2}{(\cosh \tau - \cos \sigma)^2} \, d\sigma d\tau. \tag{3}$$

Green's function satisfies

$$\Delta_{\mathbf{x}} G(\mathbf{x}_0, \mathbf{x}) = -\delta(\mathbf{x} - \mathbf{x}_0) \qquad \mathbf{x} \in C, \tag{4}$$

with conditions on the boundaries of C. We consider two cases.

- $G_1(\mathbf{x}_0, \mathbf{x})$ is the solution of (4), constrained to be zero when $\tau = \tau_2$ and to have normal derivative zero when $\tau = \tau_1$. The corresponding time obtained from (3) is the mean time for a diffusing particle to reach the boundary of the circle of radius R, when the boundary of the inclusion is reflecting.

- $G_2(\mathbf{x}_0, \mathbf{x})$ is the solution of (4), constrained to be zero when $\tau = \tau_1$ and to have normal derivative zero when $\tau = \tau_2$. The corresponding time obtained from (3) is the mean time for a diffusing particle to reach the inclusion, when the boundary of the circle of radius R is reflecting.

In terms of (τ, σ), the bipolar coordinate representation of $\mathbf{x}$, and (τ_0, σ_0), the representation of $\mathbf{x}_0$, we define $\tau_A = \min(\tau, \tau_0) - \tau_2$, $\tau_B = \tau_1 - \max(\tau, \tau_0)$ and $\theta = |\sigma - \sigma_0| - \pi$, where $-\pi < \theta \leq \pi$.

Equivalence of series

Two different series expressions exist for G_1 and G_2. Based on the form used by Heyda [36], we can write [14]

$$2\pi G_1(\mathbf{x}_0, \mathbf{x}) = \tau_A + \sum_{m=1}^{\infty} \frac{2}{m} \frac{\sinh m\tau_A \cosh m\tau_B}{\cosh m(\tau_1 - \tau_2)} \cos m\theta \tag{5}$$

and

$$2\pi G_2(\mathbf{x}_0, \mathbf{x}) = \tau_B + \sum_{m=1}^{\infty} \frac{2}{m} \frac{\sinh m\tau_B \cosh m\tau_A}{\cosh m(\tau_1 - \tau_2)} \cos m\theta. \tag{6}$$

A different summation, developed by Liemert [29], may be modified to the case of one absorbing and one reflecting boundary to yield

$$2\pi G_1(\mathbf{x}_0, \mathbf{x}) = \sum_{n=0}^{\infty} \frac{4}{2n+1} \frac{\sin\left(\lambda_n(\tau - \tau_2)\right) \sin\left(\lambda_n(\tau_0 - \tau_2)\right)}{\sinh \lambda_n \pi} \cosh \lambda_n \theta, \tag{7}$$

and

$$2\pi G_2(\mathbf{x}_0, \mathbf{x}) = \sum_{n=0}^{\infty} \frac{4}{2n+1} \frac{\sin\left(\lambda_n(\tau_1 - \tau)\right) \sin\left(\lambda_n(\tau_1 - \tau_0)\right)}{\sinh \lambda_n \pi} \cosh \lambda_n \theta, \tag{8}$$

where

$$\lambda_n = \frac{(2n+1)\pi}{2(\tau_1 - \tau_2)}. \tag{9}$$

Our first aim is to demonstrate that these two expressions, superficially very different, are equivalent. To do so, we seek to write (5) in the form

$$2\pi G_1(\mathbf{x}_0, \mathbf{x}) = \sum_{l=0}^{\infty} A_l \sin(\lambda_l(\tau - \tau_2)),$$

where

$$A_l = \frac{4\pi}{\tau_1 - \tau_2} \int_{\tau_2}^{\tau_1} G_1(\mathbf{x}_0, \mathbf{x}) \sin\left(\lambda_l(\tau - \tau_2)\right) \mathrm{d}\tau.$$

Thus

$$A_l = \frac{8}{\pi} \frac{\lambda_l}{2l+1} \left(\frac{1}{2\lambda_l^2} + \sum_{m=1}^{\infty} \frac{\cos m\theta}{\lambda_l^2 + m^2} \right) \sin \lambda_l(\tau_0 - \tau_2).$$

Using

$$\frac{\cosh \lambda_m \theta}{\sinh \lambda_m \pi} = \frac{2\lambda_m}{\pi} \left(\frac{1}{2\lambda_m^2} + \sum_{n=1}^{\infty} \frac{\cos n\theta}{\lambda_m^2 + n^2} \right),$$

we find

$$A_l = \frac{4}{2l+1} \frac{\cosh \lambda_l \theta}{\sinh \lambda_l \pi} \sin \lambda_l(\tau_0 - \tau_2),$$

which is consistent with (7). Similarly, (6) is equivalent to (8).

Evaluation without series

To obtain closed expressions that are not series expansions, we rearrange the summand in (7), using [29]

$$4 \sin \left(\lambda_n(\tau - \tau_2) \right) \sin \left(\lambda_n(\tau_0 - \tau_2) \right) \cosh \lambda_n \theta$$
$$= \Re(e^{i(2n+1)\beta} + e^{-i(2n+1)\beta} - e^{i(2n+1)\alpha} - e^{-i(2n+1)\alpha}),$$

where $\Re(z)$ is the real part of z,

$$\alpha = \frac{\pi}{2} \frac{\tau + \tau_0 - 2\tau_2 + i\theta}{\tau_1 - \tau_2}, \qquad \beta = \frac{\pi}{2} \frac{\tau - \tau_0 + i\theta}{\tau_1 - \tau_2}, \tag{10}$$

and

$$\sinh(\lambda_n \pi) = \frac{1 - q^{2(2n+1)}}{2q^{2n+1}} \quad \text{where} \quad q = \exp\left(-\frac{\pi^2}{2(\tau_1 - \tau_2)} \right). \tag{11}$$

Then (7) is written [29]

$$2\pi G_1(\mathbf{x}_0, \mathbf{x}) = \sum_{n=0}^{\infty} \sum_{k=1}^{\infty} \frac{q^{(2k-1)(2n+1)}}{2n+1} 2\Re\left(e^{i(2n+1)\beta} + e^{-i(2n+1)\beta} - e^{i(2n+1)\alpha} - e^{-i(2n+1)\alpha} \right).$$

When $|z| < 1$,

$$2\Re\left(\sum_{n=0}^{\infty} \frac{z^{2n+1}}{2n+1} \right) = \log\left| \frac{1+z}{1-z} \right|.$$

Therefore

$$\begin{aligned}
2\pi G_1(\mathbf{x}_0, \mathbf{x}) &= \sum_{k=1}^{\infty} \log\left| \frac{1 + q^{2k-1}e^{i\beta}}{1 - q^{2k-1}e^{i\beta}} \frac{1 + q^{2k-1}e^{-i\beta}}{1 - q^{2k-1}e^{-i\beta}} \frac{1 - q^{2k-1}e^{i\alpha}}{1 + q^{2k-1}e^{i\alpha}} \frac{1 - q^{2k-1}e^{-i\alpha}}{1 + q^{2k-1}e^{-i\alpha}} \right| \\
&= \sum_{k=1}^{\infty} \log\frac{|1 + 2q^{2k-1}\cos\beta + q^{4k-2}| \, |1 - 2q^{2k-1}\cos\alpha + q^{4k-2}|}{|1 - 2q^{2k-1}\cos\beta + q^{4k-2}| \, |1 + 2q^{2k-1}\cos\alpha + q^{4k-2}|} \\
&= \log\left| \frac{\vartheta_3(\beta/2, q)\vartheta_4(\alpha/2, q)}{\vartheta_4(\beta/2, q)\vartheta_3(\alpha/2, q)} \right|,
\end{aligned} \tag{12}$$

where $\vartheta_3(z, q)$ and $\vartheta_4(z, q)$ are Jacobi theta functions [29, 37]. Similarly,

$$2\pi G_2(\mathbf{x}_0, \mathbf{x}) = \log\left| \frac{\vartheta_3(\beta_2/2, q)\vartheta_4(\alpha_2/2, q)}{\vartheta_4(\beta_2/2, q)\vartheta_3(\alpha_2/2, q)} \right|, \tag{13}$$

where

$$\alpha_2 = \frac{\pi}{2} \frac{2\tau_1 - \tau - \tau_0 + i\theta}{\tau_1 - \tau_2} \quad \text{and} \quad \beta_2 = \frac{\pi}{2} \frac{\tau_0 - \tau + i\theta}{\tau_1 - \tau_2}.$$

In Fig 2, the dependence of $G_1(\mathbf{x}_0, \mathbf{x})$ and $G_2(\mathbf{x}_0, \mathbf{x})$ on $\mathbf{x}$ is shown, with $\mathbf{x}_0$ fixed, when $c = 0.5$ and $a = 0.2$. We use the closed expressions (12) and (13). Jacobi functions are available in many software packages; we give an example in the S1 Code.
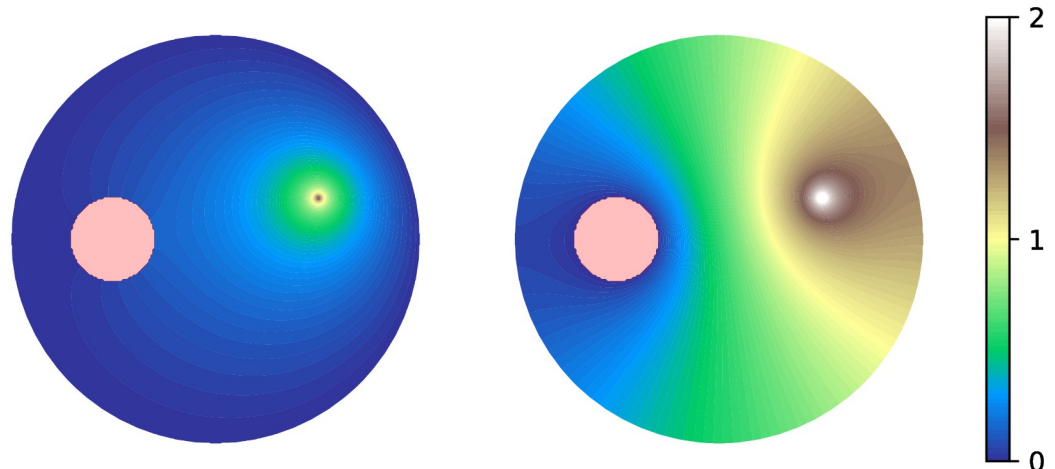
Fig 2. Exact Green's functions. Left: $G_1(\mathbf{x}_0, \mathbf{x})$. The boundary of the unit circle is absorbing, the boundary of the inclusion is reflecting. Right: $G_2(\mathbf{x}_0, \mathbf{x})$. The boundary of the unit circle is reflecting, the boundary of the inclusion is absorbing. The initial position of the diffusing particle, $\mathbf{x}_0$, is displaced by $(0.5, 0.2)$ from the center of the unit disk; the inclusion has radius 0.2 and is displaced by $(−0.5, 0)$. The value of the function at $\mathbf{x}$ is the occupation density of the diffusing particle, until reaching the absorbing boundary. We use the closed expressions (12) and (13) that involve the Jacobi theta function. Python code is provided in the S1 Code.

If truncated at a finite number of terms, the series expressions (5)–(8) are not exact. To consider the effect of only using a finite number of terms, we define

$$2\pi G_1^{\mathrm{H}}(\mathbf{x}_0, \mathbf{x}, n) = \tau_{\mathrm{A}} + \sum_{m=1}^{n} \frac{2}{m} \frac{\sinh m\tau_{\mathrm{A}} \cosh m\tau_B}{\cosh m(\tau_1 - \tau_2)} \cos m\theta \tag{14}$$

$$2\pi G_1^{\mathrm{L}}(\mathbf{x}_0, \mathbf{x}, n) = \sum_{m=0}^{n} \frac{4}{2m+1} \frac{\sin(\lambda_m(\tau - \tau_2))\sin(\lambda_m(\tau_0 - \tau_2))}{\sinh \lambda_m \pi} \cosh \lambda_m \theta, \tag{15}$$

and similary $G_2^{\mathrm{H}}(\mathbf{x}_0, \mathbf{x}, n)$ and $G_2^{\mathrm{L}}(\mathbf{x}_0, \mathbf{x}, n)$. Fig 3 shows how the error is distributed on the domain, when 20 terms in each series are used. Note that the error using (5) and (6), is largest close to $\tau = \tau_0$; the error using (7) and (8) is largest close to $\sigma = \sigma_0$. In practice, evaluating mean times by performing the integral (3) is most convenient using the forms (5) and (6).

Conclusion

Green's functions are used to calculate mean hitting or exit times of Brownian particles in confined domains whose boundaries are reflecting in some places and absorbing in others. We give exact results in two dimensions when the domain is a circle (cellular surface) with a circular inclusion (cellular nucleus). Two different types of series expression emerge when using bipolar coordinates. We sum the series to yield a closed expression involving Jacobi theta functions. The methodology of this paper can be extended to three dimensions with bispherical coordinates [27]. Transformations using bipolar and bispherical coordinates have only yielded exact results when there is a single inclusion on a circular domain. Nevertheless, exact results are useful complements to current numerical and analytical methods, accurate in certain limits, for confined diffusion with narrow exits or multiple targets [18–20, 38].
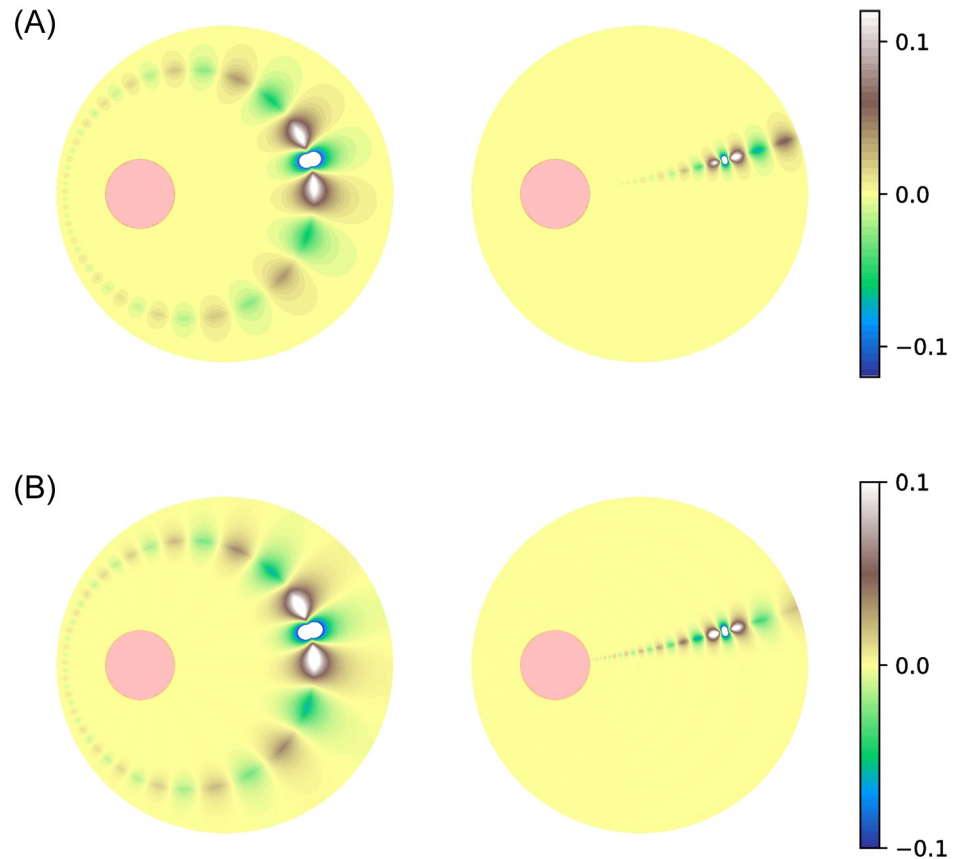
Fig 3. Dependence of truncation errors in Green's functions on position x. The inclusion is the red disk, displaced by $(-0.5, 0)$ with respect to the centre of the unit circle, and the initial position $\mathbf{x}_0$ of the diffusing particle, is displaced by $(0.5, 0.2)$. Upper left: $G_1(\mathbf{x}_0, \mathbf{x}) - G_1^H(\mathbf{x}_0, \mathbf{x}, 20)$. Upper right: $G_1(\mathbf{x}_0, \mathbf{x}) - G_1^L(\mathbf{x}_0, \mathbf{x}, 20)$. Lower left: $G_2(\mathbf{x}_0, \mathbf{x}) - G_2^H(\mathbf{x}_0, \mathbf{x}, 20)$. Lower right: $G_2(\mathbf{x}_0, \mathbf{x}) - G_2^L(\mathbf{x}_0, \mathbf{x}, 20)$.

https://doi.org/10.1371/journal.pone.0265935.g003

Supporting information

S1 Code.
(PDF)

Author Contributions

Formal analysis: Remus Stana.

Funding acquisition: Grant Lythe.

Investigation: Remus Stana, Grant Lythe.

Methodology: Grant Lythe.

Supervision: Grant Lythe.

Writing – original draft: Remus Stana, Grant Lythe.

Writing – review & editing: Remus Stana, Grant Lythe.

References

1. Berg HC. Random walks in biology. Princeton University Press; 1993.

2. Bressloff PC, Newby JM. Stochastic models of intracellular transport. Reviews of Modern Physics. 2013; 85(1):135. https://doi.org/10.1103/RevModPhys.85.135

3. Schuss Z. Brownian dynamics at boundaries and interfaces. Springer; 2015.

4. Grebenkov DS, Holcman D, Metzler R. Preface: new trends in first-passage methods and applications in the life sciences and engineering. Journal of Physics A: Mathematical and Theoretical. 2020; 53 (19):190301. https://doi.org/10.1088/1751-8121/ab81d5

5. Morse PM, Feshbach H. Methods of theoretical physics. McGraw-Hill; 1953.

6. Schuss Z. Theory and applications of stochastic processes: an analytical approach. vol. 170. Springer Science & Business Media; 2009.

7. Holcman D. Stochastic processes, multiscale modeling, and numerical methods for computational cellular biology. Springer; 2017.

8. Grebenkov DS, Metzler R, Oshanin G. Effects of the target aspect ratio and intrinsic reactivity onto diffusive search in bounded domains. New Journal of Physics. 2017; 19(10):103025. https://doi.org/10.1088/1367-2630/aa8ed9

9. Barton G. Elements of Green's functions and propagation: potentials, diffusion, and waves. Oxford University Press; 1989.

10. Redner S. A guide to first-passage processes. Cambridge University Press; 2001.

11. Stirzaker D, et al. Stochastic processes and models. OUP Catalogue. 2005.

12. Prüstel T, Meier-Schellersheim M. Exact Green's function of the reversible diffusion-influenced reaction for an isolated pair in two dimensions. Journal of Chemical Physics. 2012; 137(5):054104. https://doi.org/10.1063/1.4737662 PMID: 22894329

13. Cobbold CA, Lutscher F. Mean occupancy time: linking mechanistic movement models, population dynamics and landscape ecology to population persistence. Journal of mathematical biology. 2014; 68 (3):549–579. https://doi.org/10.1007/s00285-013-0642-1 PMID: 23334354

14. Stana R, Lythe G, Molina-París C. Diffusion in a disk with a circular inclusion. SIAM Journal on Applied Mathematics. 2021; 81:1287. https://doi.org/10.1137/20M1351394

15. Chevalier C, Bénichou O, Meyer B, Voituriez R. First-passage quantities of Brownian motion in a bounded domain with multiple targets: a unified approach. Journal of Physics A: Mathematical and Theoretical. 2010; 44(2):025002. https://doi.org/10.1088/1751-8113/44/2/025002

16. Delgado MI, Ward MJ, Coombs D. Conditional mean first passage times to small traps in a 3-D domain with a sticky boundary: Applications to T-cell searching behavior in lymph nodes. Multiscale Modeling and Simulation. 2015; 13(4):1224–1258. https://doi.org/10.1137/140978314

17. Erban R, Chapman SJ. Stochastic modelling of reaction–diffusion processes. vol. 60. Cambridge University Press; 2019.

18. Condamin S, Bénichou O, Moreau M. Random walks and Brownian motion: A method of computation for first-passage times and related quantities in confined geometries. Physical Review E. 2007; 75 (2):021111. https://doi.org/10.1103/PhysRevE.75.021111 PMID: 17358317

19. Kurella V, Tzou JC, Coombs D, Ward MJ. Asymptotic analysis of first passage time problems inspired by ecology. Bulletin of Mathematical Biology. 2015; 77(1):83–125. https://doi.org/10.1007/s11538-014-0053-5 PMID: 25515029

20. Paquin-Lefebvre F, Iyaniwura S, Ward M. Asymptotics of the principal eigenvalue of the Laplacian in 2D periodic domains with small traps. European Journal of Applied Mathematics. 2020; p. 1–28.

21. Iyaniwura S, Ward M. Asymptotic analysis for the mean first passage time in finite or spatially periodic 2D domains with a cluster of small traps. The ANZIAM Journal. 2021; p. 1–22. https://doi.org/10.21914/anziamj.v63.15976

22. Iyaniwura SA, Wong T, Macdonald CB, Ward MJ. Optimization of the mean first passage time in near-disk and elliptical domains in 2-D with small absorbing traps. SIAM Review. 2021; 63(3):525–555. https://doi.org/10.1137/20M1332396

23. Chen JT, Tsai MH, Liu CS. Conformal mapping and bipolar coordinate for eccentric Laplace problems. Computer Applications in Engineering Education. 2009; 17(3):314–322. https://doi.org/10.1002/cae.20208

24. Priestley HA. Introduction to complex analysis. OUP Oxford; 2003.

25. Carrier GF, Pearson CE. Partial differential equations: theory and technique. Academic Press; 2014.

26. Chen J, Shieh H, Lee Y, Lee J. Bipolar coordinates, image method and the method of fundamental solutions for Green's functions of Laplace problems containing circular boundaries. Engineering Analysis with Boundary Elements. 2011; 35(2):236–243. https://doi.org/10.1016/j.enganabound.2010.08.008

27. Stana RL. Diffusive transport: theory and application. University of Leeds; 2020.

28. Chen JT, Lee JW, Shieh HC. A Green's Function for the Domain Bounded by Nonconcentric Spheres. Journal of Applied Mechanics. 2013; 80(1):014503. https://doi.org/10.1115/1.4007071

29. Liemert A. The Green's function of the Poisson equation on the non-concentric annular region. Journal of Electrostatics. 2014; 72(4):347–351. https://doi.org/10.1016/j.elstat.2014.03.006

30. Ward MJ, Keller JB. Strong localized perturbations of eigenvalue problems. SIAM Journal on Applied Mathematics. 1993; 53(3):770–798. https://doi.org/10.1137/0153038

31. Schuss Z, Singer A, Holcman D. The narrow escape problem for diffusion in cellular microdomains. Proceedings of the National Academy of Sciences. 2007; 104(41):16098–16103. https://doi.org/10.1073/pnas.0706599104 PMID: 17901203

32. Coombs D, Straube R, Ward M. Diffusion on a sphere with localized traps: mean first passage time, eigenvalue asymptotics, and Fekete points. SIAM Journal of Applied Math. 2009; 70(1):302–332. https://doi.org/10.1137/080733280

33. Cheviakov A, Ward M. Optimizing the Fundamental Eigenvalue of the Laplacian in a Sphere with Interior Traps, submitted. European J Appl Math. 2009.

34. Bénichou O, Chevalier C, Klafter J, Meyer B, Voituriez R. Geometry-controlled kinetics. Nature Chemistry. 2010; 2(6):472. https://doi.org/10.1038/nchem.622 PMID: 20489716

35. Holcman D, Schuss Z. Stochastic narrow escape in molecular and cellular biology. Analysis and Applications Springer, New York. 2015.

36. Heyda JF. A Green's function solution for the case of laminar incompressible flow between non-concentric circular cylinders. Journal of the Franklin Institute. 1959; 267(1):25–34. https://doi.org/10.1016/0016-0032(59)90034-1

37. Whittaker ET, Watson GN. A course of modern analysis. Fourth edition. ed. Cambridge: University Press; 1927.

38. Singer A, Schuss Z, Holcman D. Narrow escape, Part II: The circular disk. Journal of Statistical Physics. 2006; 122(3):465–489. https://doi.org/10.1007/s10955-005-8027-5